TRITA-ALP-2000-01
Report
ISSN 1103-6613
ISRN KTH/ALP/R--00/1--SE

POLAR UVI Observations of Auroral Oval Intensifications During a Transpolar Arc Event on December 7, 1996

J. A. Cumnock[1,2], J. F. Spann[3], G. A. Germany[4], L. G. Blomberg[1]
W. R. Coley[2], C. R. Clauer[5], M. J. Brittnacher[6]

Stockholm, March 2000

[1] Alfvén Laboratory, Royal Institute of Technology, Stockholm, Sweden
[2] William B. Hanson Center for Space Sciences, University of Texas at Dallas, Richardson, TX
[3] NASA Marshall Space Flight Center, Huntsville, AL
[4] Center for Space Plasma and Aeronomic Research, University of Alabama, Huntsville, AL
[5] Space Physics Research Lab, University of Michigan, Ann Arbor, MI
[6] Geophysics Department, University of Washington, Seattle, WA

POLAR UVI Observations of Auroral Oval Intensifications During a Transpolar Arc Event on December 7, 1996

J. A. Cumnock, J. F. Spann, G. A. Germany, L. G. Blomberg
W. R. Coley, C. R. Clauer, M. J. Brittnacher

Abstract

The evolution of the northern hemisphere aurora is examined during a time when the IMF makes three brief southward excursions after a change in the sign of B_y during an extended period of northward IMF. POLAR UVI provides images of the aurora while DMSP F13 and F14 provide in situ measurements of precipitating particles, ionospheric plasma flows and ion density.

Three different intensifications located in the nightside auroral oval occur during northward turnings of the IMF after brief periods of southward IMF. Spatial expansion, intensity of emissions and their duration are related to the length of time the IMF is southward prior to the northward turning. Thus the longer the period of enhanced magnetospheric convection the more intense the ionospheric response. Observations of a transpolar arc indicate that when the transpolar arc reaches highest latitudes it is located on a spatially narrow region of closed field lines, which extends along the noon-midnight meridian.

UV observations indicate a connection between the transpolar arc and the nightside auroral enhancements. Precipitating particles associated with both features are attributed to a plasma sheet boundary layer source in the magnetotail implying a magnetospheric connection between the transpolar arc and the nightside auroral oval intensification.

1. Introduction

Energy transfer from the solar wind to the Earth's magnetosphere is primarily dependent on the orientation of the interplanetary magnetic field (IMF). When the IMF is directed southward more of the Earth's geomagnetic field lines connect to the IMF than when it is northward, resulting in more efficient energy transfer from the solar wind through the magnetosphere and into the ionosphere. The southward IMF configuration increases magnetospheric convection, which results in a spatially larger auroral oval. Intermittent release of the energy stored in the magnetosphere through internal instabilities and/or external changes in the IMF cause increased auroral activity. This includes a wide variety of auroral phenomena of differing intensities and spatial extents, which are generally classified as substorms. Satellite imagers provide global images of substorm evolution [*Craven and Frank*, 1985; *Hones et al.*, 1987; *Brittnacher et al.*, 1999]. Ground based observations include enhanced westward ionospheric currents which cause a large negative change in the northward component of the ground magnetic field [*Akasofu*, 1968] and suddenly enhanced Pi2 micropulsations [*Rostoker*, 1968].

During intervals of northward IMF, the magnetosphere has a more closed topology resulting in an auroral oval which is contracted to higher latitudes and "quiet" compared with the southward IMF aurora. However, localized regions of bright emissions on the poleward edge of the auroral oval near magnetic midnight, in a previously quiet auroral oval, have often been observed [e.g. *Shepherd et al.*, 1987]. In addition, the northward IMF aurora often exhibits broad emission regions in the dawn and dusk sectors that can spread poleward to very high latitudes. In the northern hemisphere an emission region forms on the duskside (dawnside) of the noon-midnight meridian when B_y is positive (negative) [*Hones et al.*, 1989]. When average B_y is near zero, emission regions often occur on both the dawn and dusk sides of the auroral oval resulting in a "teardrop shaped" region near the pole which is void of auroral emissions [*Murphree et al.*, 1982]; this pattern is sometimes referred to as the "horse-collar aurora" [*Hones et al.*, 1989]. During predominantly northward IMF large-scale sun-aligned transpolar arcs can be observed to extend across the polar region from the local-noon sector to the midnight sector. The motion and location of the transpolar arcs are dependent on the sign of B_y, with the transpolar arcs moving toward the duskside of the noon-midnight meridian in the northern hemisphere when B_y is positive [*Huang et al.*, 1989] and toward the dawnside when B_y is negative [*Frank et al.*, 1985; *Craven and Frank*, 1991]. The auroral pattern made up of the transpolar arc and the oval has also been called "theta aurora" [*Frank et al.*, 1982]. The expanded dawn and dusk side emission

regions formed during weakly northward conditions have been reported to evolve into sun-aligned transpolar arcs located at highest latitudes [*Hones et al.*, 1989]. This evolution has been observed to require a large $+B_z/|B_y|$ ratio corresponding to a change in the sign of B_y, where a theta aurora is formed from an expanded dawnside (duskside) emission region when B_y changes from negative to positive (positive to negative) [*Cumnock et al*., 1997]. Models produce theta aurora with a sign change in IMF B_y [*Akasofu and Roederer*, 1983; *Chang et al*., 1998; *Kullen*, 2000]; and with sign changes in both IMF B_y and B_z [*Newell and Meng*, 1995].

Northward IMF phenomena such as theta and horse collar aurora have been observed to occur simultaneously with auroral intensifications and substorms, which occur in the nightside oval and are normally associated with more active magnetospheric conditions [*Murphree et al*., 1987; *Murphree et al*., 1994; *Henderson et al*., 1996]. It is unclear what triggers these intensifications and/or substorms, especially in the quiet auroral oval. Some observations indicate that substorms may be triggered by a reduction in the large-scale electric field imparted to the magnetosphere from the solar wind which results from a northward turning of the IMF or a reduction in the magnitude of B_y (or internal magnetospheric instabilities possibly caused by a changing IMF) [*Lyons*, 1995]. Two features seen in previous observations of intensifications in the nightside auroral oval where sun-aligned arcs intersect the oval are of particular interest. One is the simultaneous motion of arc and intensification; the second is the intensification of the arc as the oval intensification fades. This implies a direct relationship between the oval intensification and connected polar arc [*Murphree et al*., 1987]. *Weygand et al.* [*submitted* 1999] summarize previous observations of simultaneously occurring polar arcs and substorms and discuss possible magnetospheric mappings. However, previous investigations do not consider the type of polar arc, its dependence on the IMF, how it was formed or its stability, all of which influence the interaction (constructive or destructive) between transpolar arc and substorm.

The poleward edges (arcs) of the dawn and dusk emission regions are generally assumed to mark the boundary between open and closed field lines [*Murphree et al*., 1982; *Frank et al*., 1986; *Lassen et al*., 1988]. Previous studies of energetic particle data indicate that the configuration of the magnetosphere during a theta aurora involves a topological change permitting closed field lines to expand to higher latitudes in one of two configurations: (1) isolated structures within a poleward expanded magnetospheric boundary layer (LLBL, PSBL) [*Meng*, 1981; *Eliasson et al*., 1987; *Lundin et al*., 1991]; or (2) a bifurcation of the magnetotail lobe by closed field lines [*Bythrow et al.*, 1985; *Frank et al*., 1986]. Both configurations produce an isolated region of

energetic electrons and ions (plasma sheet-like particles) at highest latitudes surrounded by precipitation regions characterized by polar rain electrons and void of ions (or below instrument detection).

In this paper we describe the evolution of the global aurora during a time when the IMF makes three brief southward excursions after a change in the sign of B_y during an extended period of northward IMF. The resulting auroral pattern, made up of a transpolar arc and substorm, is a rare occurrence and not explained by current substorm and theta auroral models. The evolution of the aurora and the effects of the changes in the IMF are considered. We also examine energetic particle signatures and ion density in the ionosphere.

2. Observations

The Ultraviolet Imager (UVI) experiment [*Torr et al.*, 1995] on the POLAR spacecraft provides global images of the aurora. POLAR was launched on February 24, 1996 into an 86-degree inclination orbit, with an apogee of 9 R_E in the northern hemisphere, and a perigee of 1.8 R_E. The UVI experiment is one of four instruments mounted on a despun platform which can be oriented along one axis. The UV imager, with an 8-degree field of view, can image the entire auroral oval above 60 degrees north latitude at spacecraft altitudes greater than 6 R_E. The instrument is able to resolve 0.5 degrees in latitude at apogee; thus a single pixel projected to 100 km altitude from apogee is approximately 50x50 km. Filter 4 detected Lyman-Birge-Hopfield molecular nitrogen emissions in the 140-160 nm spectral region. For this event, the UV imager was in a mode where 36-second integration period images of the northern hemisphere aurora using filter 4 were made at approximately 3-minute intervals. We examine a series of 46 images taken between 16:27 and 19:03 UT on December 7, 1996.

False color images of auroral luminosities are presented in Figures 1, 2 and 3, with a linear color scale (with white representing no intensity and red the highest intensity) indicating photon flux collected in the instrument aperture. In Figures 1 and 2 the scale extends to 20 photons/cm^{2}s. In Figure 3 the scale extends to 30 photons/cm^{2}s in order to display the greater range of emissions during this period. The images are plotted utilizing the magnetic apex coordinate system [*Richmond*, 1995] with corresponding magnetic local time (MLT). Plot labels include year, month, day, hour, minute and second, with the time tag denoting the middle of the integration period. Note that throughout this time period the dayside oval is not in the imager field of view.

Spacecraft wobble is in the 3 to 15 MLT direction over 10 pixels (out of 228 pixels) and has no impact on the conclusions presented in this paper.

Figure 4 shows 1-minute averages of solar wind density, velocity and the three components and magnitude of the IMF in the geocentric solar magnetospheric (GSM) coordinate system obtained by the WIND SWE experiment [*Ogilvie et al.*, 1995] and MFI experiment [*Lepping et al.*, 1995]. Labels at the bottom of the figure are UT, labels at the top are corresponding POLAR UV image time tags which have been time-shifted with respect to UT to account for transit time of the IMF measured at WIND to when the effects are seen in the Earth's ionosphere. For the period under study WIND was located at approximately X=44, Y=-48, Z=5 R_E GSM. This translates into an estimated time delay between the IMF measurement and that appropriate at the magnetopause (~10 R_E in front of the Earth) of approximately 11 minutes assuming the IMF propagates radially away from the sun. GEOTAIL, located at approximately X=-20, Y=-20, Z=0 GSM, shows very similar IMF conditions with an estimated lag time between WIND and GEOTAIL of between 16 and 20 minutes depending on solar wind velocity. The effects are expected to be seen in the ionosphere after an additional internal magnetospheric delay. We estimate a total delay time between WIND and the effect of the changing IMF on the nightside auroral oval to be about 25 minutes.

IMF Influence on the Auroral Oval Intensifications

Prior to about 15:45 UT IMF B_x and B_z are positive and IMF B_y is negative. IMF B_z has been, on average, less than or equal to the magnitude of negative B_y for about 6 hours. Previous observations indicate that the dawnside of the auroral oval would expand poleward for these IMF conditions [*Hones et al.*, 1989].

At about 15:45 UT B_y changes from negative to positive. It is during such IMF B_y changes that previous investigations indicate that the poleward edge of the dawnside emission region would brighten and begin separating from the dawnside oval, eventually forming a theta aurora if B_y remains positive [*Cumnock et al.*, 1997]. Note that the solar wind velocity and density are increasing slightly throughout the time period of interest, however the solar wind velocity (~370 to 390 km/s) is much less than the 500 to 700 km/s usually associated with theta aurora.

In the first UV image taken at 16:27 UT (Figure 1), the transpolar arc is in the process of separating from the dawnside emission region. These are typical quiet auroral emissions of approximately 7 photons/cm^{2}s. Note that with B_y positive an expanded duskside emission region should begin forming, however this region is not in the field of view of the POLAR UV imager. After the transpolar arc begins forming, IMF B_z makes three southward excursions which last 20, 30 and 50 minutes (with minimum values of -4, -3 and -5 nT) respectively, before the IMF B_z turns northward at WIND (16:16, 17:03 and 18:04 UT, marked by vertical lines in Figure 4). Similar IMF features are seen by GEOTAIL with a delay of about 20, 17 and 16 minutes respectively.

The next image of interest occurs at 16:41 UT. The imager has been reaimed resulting in a more restricted view of the nightside oval. The first northward IMF turning occurs simultaneously with a small increase in B_x and decrease in B_y. Note first vertical line in Figure 4. This change in the IMF is correlated with an intensification in the nightside auroral oval at 16:41 UT. Note that this assumes about a 15-minute delay in the effects of a changing IMF at the magnetopause on the nightside aurora. Although the propagation time of the solar wind through the bow shock and the magnetosheath cannot be calculated, previous investigations of IMF effects on ionospheric convection report that intramagnetospheric processes introduce a time delay of about 15 to 20 minutes [*Feldstein et al.*, 1996]. The enhancement in the nightside oval occurs at approximately 1 MLT just westward of where the transpolar arc intersects the oval. This intensification is by far the brightest feature in the field of view of the UV imager with a peak intensity of about 20 photons/cm^{2}s. During the next 5 images (16:44-16:56 UT) the enhancement propagates westward expanding over 2 hours MLT (with emissions 15 photons/cm^{2}s). The transpolar arc emissions brighten and the transpolar arc moves duskward (as expected for positive B_y). During the next 4 images (16:59-17:08 UT) an enhancement on the dayside of the transpolar arc occurs (at approximately 16:59 UT) and propagates nightward implying a connection between the transpolar arc and the dayside auroral oval and their sources. The transpolar arc continues to move duskward during this time period. In the next 6 images (17:12 UT Figure 1 through 17:27 UT Figure 2) the enhancements in the transpolar arc fade and it continues to move duskward until it is aligned along the noon-midnight meridian. The image at 17:27 UT fits the classic description of a theta aurora [*Frank et al.*, 1982; 1986]. Note that the transpolar arc lacks the hook shaped attachment to the nightside oval typical of many theta aurora.

The second enhancement, seen in the UV image at 17:30 UT, is more intense and has features associated with the expansive phase of an optical substorm. It is located at about the same MLT and at slightly lower latitudes than the previous enhancement, however now the transpolar arc is aligned along the noon-midnight meridian, on the duskside of the intensification. This event is correlated with a northward turning of the IMF at 17:03 following approximately 30 minutes of southward IMF. Note second vertical line in Figure 4. The intensification appears to be the onset of an optical substorm, identified by the formation of an intensified region or "eye" which expands poleward and encompasses well defined surge-like features both eastward and westward of the original intensification [*Craven and Frank*, 1985; *Rostoker et al*., 1987; *Murphree et al*., 1991]. In addition, Pi2 pulsations are seen by the 210 meridian chain. The IMF at WIND turns southward again at 17:12 UT and remains southward for about 50 minutes coinciding with the continued expansion of the substorm-like event (17:33-18:10 UT, Figure 2). The enhanced region brightens and expands east-west with more westward expansion than eastward expansion over at least 9 hours MLT (with emissions 15 photons/cm^{2}s). Peak intensities of about 100 photons/cm^{2}s occur at 17:39 UT. There is no equatorward expansion but there is an approximately 3-degree poleward expansion at 1-2 MLT resulting in a total latitude width of about 7 degrees. Enhancements also occur in the transpolar arc, propagating in the midnight to noon direction. Even though the IMF is southward the transpolar arc continues to move duskward while B_y remains positive (UV images until about 17:58 UT). The transpolar arc fades shortly thereafter having persisted for approximately 30 minutes after the IMF turns southward.

The onset of a much larger substorm occurs at about 18:29 UT after approximately 50 minutes of southward IMF during which IMF B_x is negative, which favors connection of the IMF to the Earth's geomagnetic field x-component in the northern hemisphere. The onset at 18:29 UT is correlated with a northward turning of the IMF at WIND at about 18:04 UT (coinciding with a change of sign of B_x from negative to positive, and a sudden decrease in the solar wind velocity). Note third vertical line in Figure 4. East-west expansion for this event covers at least 11 hours MLT, with peak intensities of about 90 photons/cm^{2}s occurring at 18:35 UT. Very little equatorward expansion is apparent but there is a poleward expansion of about 7 degrees resulting in a latitudinal width of the nightside oval of about 11 degrees. Pi2 pulsations are also seen in this event.

The three events are correlated with northward turnings of the IMF and are consistent with the view that substorm-like events can be triggered by northward turnings of the IMF. Previous

investigations include those which present examples of isolated substorms which are triggered by northward turnings of the IMF [*Rostoker et al.*, 1983] and those which find a strong association between IMF triggers (northward turning or a reduction in the magnitude of B_y) and classical substorm onset [*Lyons et al.*, 1997].

Motion of the Transpolar Arc across the High-Latitude Polar Region

The Defense Meteorological Satellite Program's (DMSP) satellites provide measurements of precipitating particles at the beginning (1624-1637 UT) and end (1805-1818 UT) of the time period of interest. DMSP F13 passes in the dusk-to-dawn direction and DMSP F12 from 21 MLT to 10 MLT. The SSJ/4 instrument package includes curved plate electrostatic analyzers to measure electrons and ions from 32 eV to 30 keV at a rate of one complete electron and ion spectrum per second [*Hardy et al.*, 1984]. The special sensor for ions, electrons, and scintillation (SSIES) provides measurements of the horizontal plasma flow and ion density at a rate of 6 samples per second [*Greenspan et al.*, 1988]. Figures 5 and 6 show from top to bottom, (1) electron and ion integral energy flux, (2) electron and ion average energy, (3) precipitating electron spectrogram, (4) precipitating ion spectrogram, (5) cross-track horizontal plasma drift, and (6) ion density.

Figure 5 presents data from the first DMSP F13 satellite pass. The satellite passes over the transpolar arc from approximately 1631:32 to 1632:00 UT, 85 degrees MLAT, which is at about the same time as the first UV image shown in Figure 1. The transpolar arc appears to be embedded in an expanded dawnside oval (1631:32-1637:00 UT) attributed to an expansion of the plasma sheet boundary layer in the magnetosphere (ie. an expansion of the region where solar wind energy and momentum are transferred). The existence of ion precipitation indicates that the transpolar arc occurs on closed field lines and has energies typical of those attributed to a plasma sheet or plasma sheet boundary layer source in the magnetosphere. Note that the multiple arc structures seen in the particle data (for example: 1632:00-1634:00 UT) are not resolved in the UV imager data. A region of open field lines (polar rain electrons and void of ions) is seen at highest latitudes poleward of the transpolar arc from about 1629:30 to 1631:32 UT. During the same time interval the first DMSP F12 pass (not shown) is through the cusp and the afternoon auroral oval.

Also of interest is the response of the polar cap ionosphere to the presence of the transpolar arcs. The lowest panel of Figure 5 shows the ion density data. The elevated plasma densities associated with energetic particle precipitation on closed field lines in the auroral zones are evident in the 1626-1629 UT and 1631:32-1636 UT time intervals. The data gap from 1630:16 to 1631:32 UT is a region in the dark polar cap where the plasma density is less than the instrumental threshold of about 50 cm^{-3}. There is an enhancement in the ion density coincident with the transpolar arc's energetic particle signature from 1631:32 to 1632:00 UT. This is the type of density feature that in this location and in the absence of an energetic particle signature would be associated with a polar cap patch convecting over the polar cap from the dayside [*Coley and Heelis*, 1995; 1998]. In this case, however, the density enhancement is evidently a direct result of the transpolar arc.

Figure 6 presents data from the second DMSP F13 pass (101 minutes later). The satellite passes over the transpolar arc from approximately 1811:10 to 1811:40 UT, 90 degrees MLAT, and at about the same time as the last UV image shown in Figure 2. The transpolar arc has moved to highest latitudes and is very faint in the UV image; however, an arc, as well as multiple small-scale arc structures, is clearly seen in the precipitating particles on the duskside of the noon-midnight meridian. Ion density data indicate that the transpolar arc has weakened and there is only a faint suggestion that the ion density is elevated above the background levels of the polar cap (1811:10-1811:40 UT). For all DMSP passes during this time period ionospheric plasma flows are very structured as expected during positive B_z conditions in the winter hemisphere. The energetic particle data indicate that the transpolar arc is now isolated in a region of open field lines (either polar rain or void of precipitation) with the largest open region located dawnward of the transpolar arc from about 1812:20 to 1814:40 UT. The second DMSP F12 pass (not shown) indicates a spatially large open region between the transpolar arc and the duskside auroral oval (at about 21 MLT extending from 79 to 84 degrees magnetic latitude).

There is clearly an evolution during which a spatially narrow region of energetic particles (closed field lines) associated with the transpolar arc moves to highest latitudes and is embedded in a region containing particles associated with open field lines.

Mapping Ionospheric Signatures to the Magnetosphere

Difficulties in mapping the different phenomena to the magnetosphere include how the different ionospheric phenomena interact with one another and how these features can be mapped in a self-consistent manner to the magnetosphere. Particle measurements on field lines above the transpolar arc indicate that those field lines may originate in the plasma sheet boundary layer. Particles typically associated with oval-aligned arcs located in the poleward part of the nightside auroral oval have similar spectral characteristics, though are usually assigned a source region in the magnetotail closer to the earth than the source region for the transpolar arc. Thus both of these regions occur on closed field lines and may map to the plasma sheet boundary layer of the magnetotail. The auroral oval intensifications appear to enhance the transpolar arc by propagating along the nightside of the transpolar arc, in addition to spreading along the auroral oval. While transpolar arcs generally fade after 20-30 minutes of southward IMF, in the second event the nightside intensification may increase the duration of the transpolar arc. These observations imply a direct relationship between the sources of the nightside auroral oval intensification and connected transpolar arc. In this case the plasma sheet boundary layer would map to very high latitudes in the ionosphere.

3. Summary and Conclusions

In the time period studied, three different intensifications located in the nightside auroral oval are related to northward turnings of the IMF after brief periods of southward IMF. Although the first two intensifications may not be classified as classical substorms, similar mechanisms may be the cause. A reduction in the electric field imparted to the magnetosphere from the solar wind may be the essential element necessary for occurrence of enhancements of the nightside oval. During the period of southward IMF (enhanced magnetospheric convection and tail stretching) the energy required to power the substorm expansive phase is stored in the magnetotail. A northward turning of the IMF (reduced magnetospheric convection and tail "collapse") results in the release of energy stored in the magnetotail and in reconfiguration of the currents in the magnetotail. This then triggers an isolated enhancement or a magnetic substorm resulting in intensification and expansion of the nightside of the auroral oval [*Rostoker et al*., 1983]. It is unclear how much energy must be stored in the magnetotail prior to the northward turning in order to trigger a nightside auroral oval intensification (or substorm). However, it has been shown that a classical substorm may occur after more than 30 minutes of southward IMF [*Lyons et al*., 1997], which is true of the second and third intensifications in our study. Thus the longer the period of enhanced

magnetospheric convection the more active the ionospheric response. Residual convection, due to inertia, may also act to enhance the impact of a second or third period of southward IMF. The intensity of the emissions seen in the second and third intensification is about the same, although they are much greater than those seen in the first. In addition, the second and third intensifications last much longer than the first, and peak emissions persist for about 3 minutes during the second and nearly 12 minutes during the third event. Thus the spatial expansion, intensity of emissions and duration of the intensification is in some way proportional to the energy stored (i.e., magnitude and length of time the IMF is southward prior to the northward turning).

In the early stages of the theta aurora evolution, the transpolar arc is embedded in an expanded dawnside emission region related to an expanded plasma sheet in the magnetosphere which may be attributed to a twisted magnetotail. As the transpolar arc moves to highest latitudes it becomes isolated in a region of open field lines. Recent models do not explain how this configuration can be maintained for the few hours it takes the transpolar arc to evolve.

Precipitating-particle observations indicate that both the transpolar arc and substorm occur on closed field lines with a plasma sheet boundary layer source. In addition, UV images show an optical correspondence which implies a magnetospheric connection between the two features even though the transpolar arc may map to the far tail region while the substorm may map to a region of the magnetotail closer to Earth. This suggests either a common trigger mechanism and/or a common magnetospheric driver. However, recent observations indicate that to first order a change in B_y during generally positive B_z triggers formation of an isolated transpolar arc (from either the dawnside or duskside auroral oval) while a positive change in B_z triggers an intensification in the nightside auroral oval which in turn intensifies the transpolar arc. This relationship implies a closer magnetospheric connection between the drivers than previously thought.

More general conclusions about simultaneously occurring transpolar arcs and substorms cannot be drawn without an analysis of more events. This analysis must take into account where the transpolar arc was formed (nightside or dawn/duskside), when (before or during the substorm) and how stable it is. These characteristics indicate differences in where the transpolar arc maps in the magnetosphere and thus how the transpolar arc and substorm would interact.

Acknowledgements: The authors thank George Parks for providing POLAR UVI data, Fred Rich for providing the DMSP F12 and F13 SSIES and SSJ/4 data, and the NASA Space Physics Data Facility for providing WIND magnetometer and plasma data. The first author's work at the Alfvén Laboratory was supported by a KTH visiting scientist scholarship. Work at the University of Texas at Dallas was supported by NASA grants NAG5-4725 and NAG5-7309, and NSF grant ATM9814144. Work at the University of Michigan was supported by NASA Grant NAG5-7776.

References

Akasofu, S.-I., *Polar and Magnetospheric Substorms*, D. Reidel, Norwell, Mass., 1968.

Akasofu, S.-I. and M. Roederer, Polar cap arcs and the open regions, *Planet. Space Sci., 31*, 193, 1983.

Brittnacher, M., M. Fillingim, G. Parks, G. Germany, J. Spann, Polar cap area and boundary motion during substorms, *J. Geophys. Res., 104*, 12251, 1999.

Bythrow, P. F., W. J. Burke, T. A. Potemra, L. J. Zanetti, and T. Y. Lui, Ionospheric evidence for irregular reconnection and turbulent plasma flows in the magnetotail during periods of northward interplanetary magnetic field, *J. Geophys. Res., 90*, 5319, 1985.

Chang, S.-W., J. D. Scudder, J. B. Sigwarth, L. A. Frank, N. C. Maynard, W. J. Burke, W. K. Peterson, E. G. Shelley, R. Friedel, J. B. Blake, R. A. Greenwald, R. P. Lepping, G. J. Sofko, J.-P. Villain, and M. Lester, A comparison of a model for the theta aurora with observations from Polar, Wind, and SuperDARN, *J. Geophys. Res., 103*, 17367, 1998.

Coley, W. R. and R. A. Heelis, Adaptive identification and characterization of polar ionization patches, *J. Geophys. Res., 100*, 23819, 1995.

Coley, W. R. and R. A. Heelis, Structure and occurrence of polar ionisation patches, *J. Geophys. Res., 103*, 2201, 1998.

Craven, J. D., and L. A. Frank, The temporal evolution of a small auroral substorm as viewed from high altitudes with Dynamics Explorer 1, *Geophys. Res. Lett., 12*, 465, 1985.

Craven, J. D., and L. A. Frank, Diagnosis of auroral dynamics using global auroral imaging with emphasis on large-scale evolution, in *Auroral Physics*, edited by C.-I. Meng, M. J. Rycroft, and L. A. Frank, pp. 273, Cambridge Univ. Press, New York, 1991.

Cumnock, J. A., J. R. Sharber, R. A. Heelis, M. R. Hairston, and J. D. Craven, Evolution of the global aurora during positive IMF B_z and varying IMF B_y conditions, *J. Geophys. Res., 102*, 17489, 1997.

Eliasson, L., R. Lundin, and J. S. Murphree, Polar cap arcs observed by the Viking satellite, *Geophys. Res. Lett., 14*, 451, 1987.

Feldstein, Y. I., L. I. Gromova, A. E. Levitin, L. G. Blomberg, G. T. Marklund, and P.-A. Lindqvist, Electromagnetic characteristics of the high-latitude ionosphere during the various phases of magnetic substorms, *J. Geophys. Res., 101*, 19921, 1996.

Frank, L. A., J. D. Craven, J. L. Burch, and J. D. Winningham, Polar views of the Earth's aurora with Dynamics Explorer, *Geophys. Res. Lett., 9*, 1001, 1982.

Frank, L. A., J. D. Craven, and R. L. Rairden, Images of the Earth's aurora and geocorona from the Dynamics Explorer mission, *Adv. Space Res.*, 5(4), 53, 1985.

Frank, L. A., et al., The theta aurora, *J. Geophys. Res., 91*, 3177, 1986.

Greenspan, M.E., P.B. Anderson, J.M. Pelagatti, Characteristics of the Thermal plasma monitor (SSIES) for the Defense Meteorological Satellite Program (DMSP) spacecraft S8 through S10, *Tech. Rep. AFGL-TR-86-0227*, Air Force Geophys. Lab., Hanscom AFB, MA, 1988.

Hardy, D. A., L. K. Schmitt, M. S. Gussenhoven, F. J. Marshall, H. C. Yeh, T. L. Schumaker, A. Huber, and J. Pantazis, Precipitating electron and ion detectors (SSJ/4) for block S/D flights 6-10 DMSP satellites: Calibration and data presentation, *Tech. Rep. AFGL-TR-84-0317*, Air Force Geophys. Lab., Hanscom AFB, MA, 1984.

Henderson, M. G., J. S. Murphree, and J. M. Weygand, Observations of auroral substorms occurring together with pre-existing "quiet time" auroral patterns, *J. Geophys. Res., 101*, 24621, 1996.

Hones, E. W., Jr., C. D. Anger, J. Birn, J. S. Murphree, and L. L. Cogger, A study of a magnetospheric substorm recorded by the Viking auroral imager, *Geophys. Res. Lett., 14*, 411, 1987.

Hones, E. W., Jr., J. D. Craven, L. A. Frank, D. S. Evans, P. T. Newell, The horse-collar aurora: A frequent pattern of the aurora in quiet times, *Geophys. Res. Lett., 16*, 37, 1989.

Huang, C. Y., J. D. Craven, and L. A. Frank, Simultaneous observations of a theta aurora and associated magnetotail plasmas, *J. Geophys. Res., 94*, 10137, 1989.

Kullen, A., The connection between transpolar arcs and magnetotail rotation, *Geophys. Res. Lett., 27*, 73, 2000.

Lassen, K., C. Danielsen, and C.-I. Meng, Quiet-time average auroral configuration, *Planet. Space Sci., 36*, 791, 1988.

Lepping, R. P., et al., The Wind magnetic field investigation, *Space Sci. Rev., 71*, 207, 1995.

Lundin, R., L. Eliasson, and J. S. Murphree, The quiet-time aurora and the magnetospheric configuration, in *Auroral Physics*, edited by C.-I. Meng, M. J. Rycroft, and L. A. Frank, pp. 177, Cambridge Univ. Press, New York, 1991.

Lyons, L. R., A new theory for magnetospheric substorms, *J. Geophys. Res., 100*, 19069, 1995.

Lyons, L. R., G. T. Blanchard, J. C. Samson, R. P. Lepping, T. Yamamoto, and T. Moretto, *J. Geophys. Res., 102*, 27039, 1997.

Meng, C.-I., Polar cap arcs and the plasma sheet, *Geophys. Res. Lett., 8*, 273, 1981.

Murphree, J. S., C. D. Anger, and L. L. Cogger, The instantaneous relationship between polar cap and oval auroras at times of northward interplanetary magnetic field, *Can. J. Phys., 60*, 349, 1982.

Murphree, J. S., L. L. Cogger, C. D. Anger, D. D. Wallis and G. G. Shepherd, Oval intensifications associated with polar arcs, *Geophys. Res. Lett., 14*, 403, 1987.

Murphree, J. S., R. D. Elphinstone, L. L. Cogger, and D. Hearn, Viking optical substorm signatures, in Magnetospheric Substorms, *Geophys. Monogr. Ser*., vol 64, edited by J. R. Kan, T. A. Potemra, S. Kokubun, and T. Iijima, p. 241, AGU, Washington, D. C., 1991.

Murphree, J. S., J. B. Austin, D. J. Hearn, L. L. Cogger, R. D. Elphinstone, J. Woch, Satellite observations of polar arcs, *J. Atmos. Terr. Physics, 56*, 265, 1994.

Newell, P. T., and C.-I. Meng, Creation of theta-auroras: The isolation of plasma sheet fragments in the polar cap, *Science, 270*, 1338, 1995.

Ogilvie, K. W., et al., SWE, a comprehensive plasma instrument for the Wind spacecraft, *Space Sci. Rev., 71*, 55, 1995.

Richmond, A. D., Ionospheric electrodynamics using magnetic apex coordinates, *J. Geomagn. Geoelectr., 47*, 191, 1995.

Rostoker, G., Macrostructure of geomagnetic bays, *J. Geophys. Res., 73*, 4217, 1968.

Rostoker, G., Triggering of expansive phase intensifications of magnetospheric substorms by northward turnings of the interplanetary magnetic field, *J. Geophys. Res., 88*, 6981, 1983.

Rostoker, G., A. Vallance Jones, R. L. Gattinger, C. D. Anger, and J. S. Murphree, The development of the substorm expansive phase: The "eye" of the substorm, *Geophys. Res. Lett., 14*, 399, 1987.

Shepherd, G. G., C. D. Anger, J. S. Murphree and A. Vallance Jones, Auroral intensifications in the evening sector observed by the Viking ultra violet imager, *Geophys. Res. Lett., 14*, 395, 1987.

Torr, M. R., D. G. Torr, M. Zukic, R. B. Johnson, J. Ajello, P. Banks, K. Clark, K. Cole, C. Keffer, G. Parks, B. Tsurutani, J. Spann, A far ultraviolet imager for the international solar-terrestrial physics mission, *Space Sci. Rev., 71*, 329, 1995.

Weygand, J. M., J. S. Murphree, M. G. Henderson, and G. Enno, Simultaneous closed magnetic field line polar arcs and substorms, *submitted to J. Atmos. Terr. Physics*, 1999.

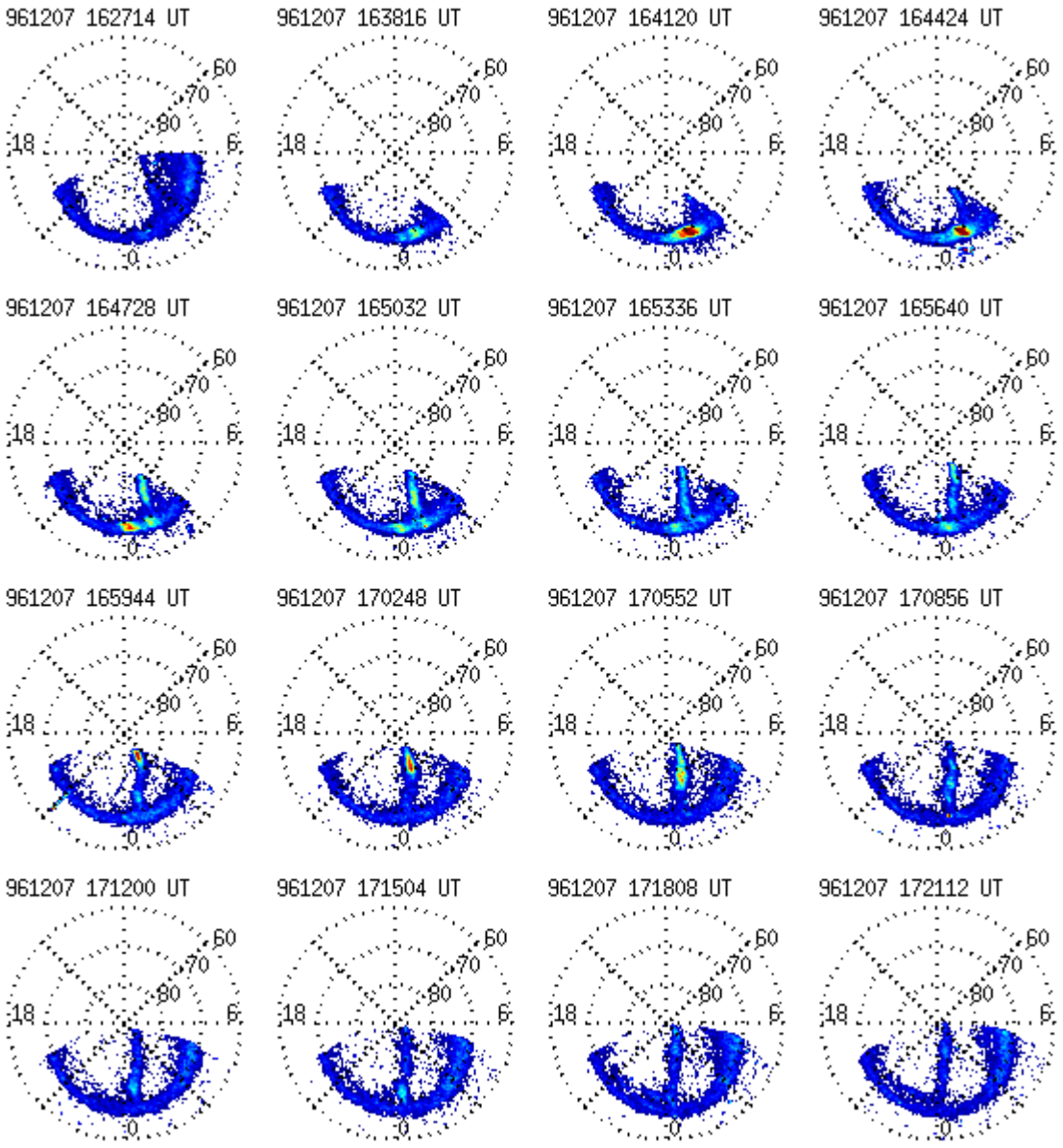

Figure 1. Images of northern hemisphere auroral luminosities (140-160 nm spectral region) from 16:27 to 17:21 UT on December 7, 1996. The linear color scale (with white representing no intensity and red the highest intensity) extends to 20 photons/cm^{2}s and indicates photon flux collected in the instrument aperture. The images are plotted utilizing the magnetic apex coordinate system [*Richmond*, 1995] with corresponding magnetic local time (MLT). Plot labels include year, month, day, hour, minute and second, with the time tag denoting the middle of the integration period. Note that throughout this time period the dayside oval is not in the imager field of view.

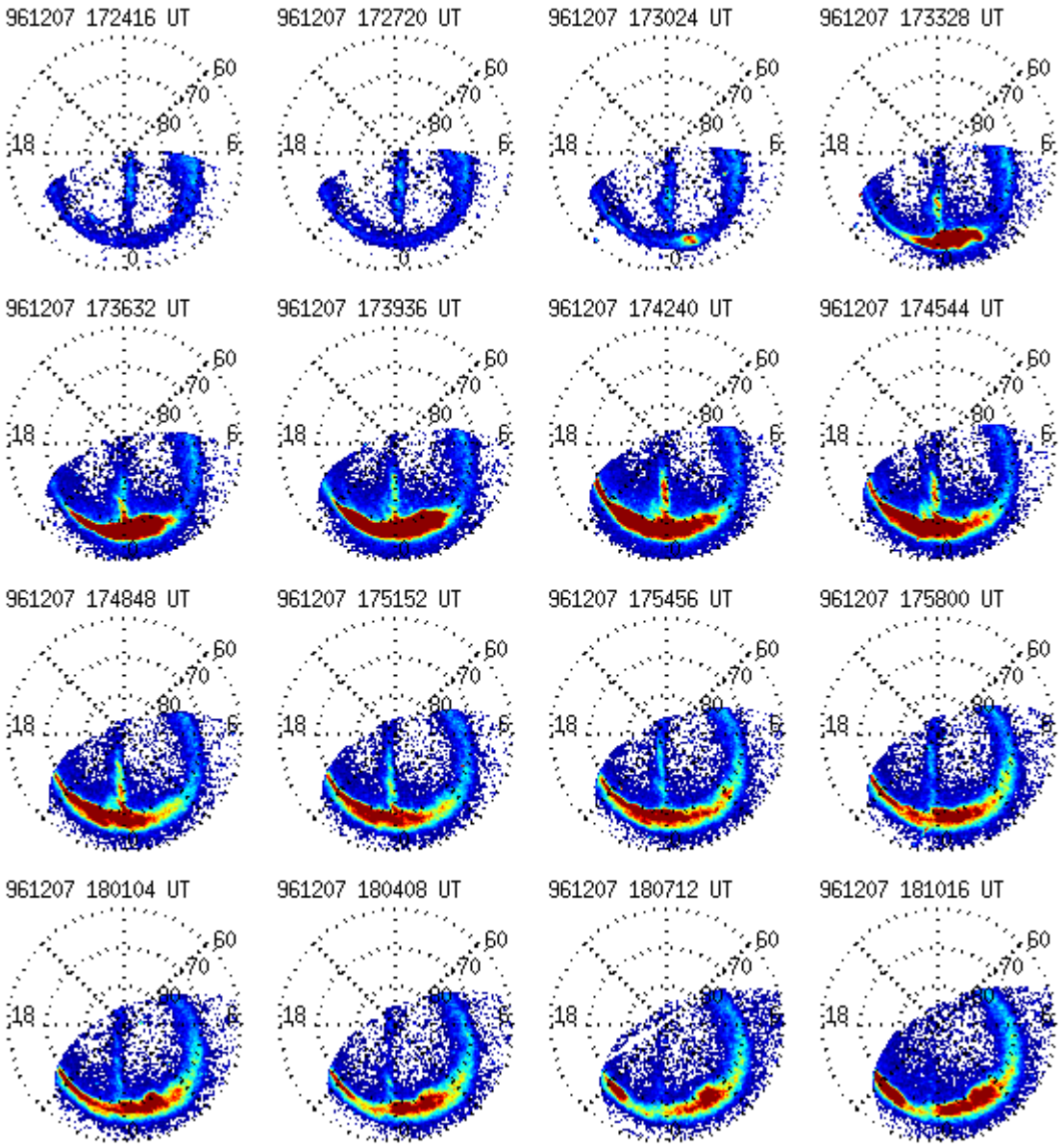

Figure 2. False color images from 17:24 to 18:10 UT on December 7, 1996. Same format as Figure 1.

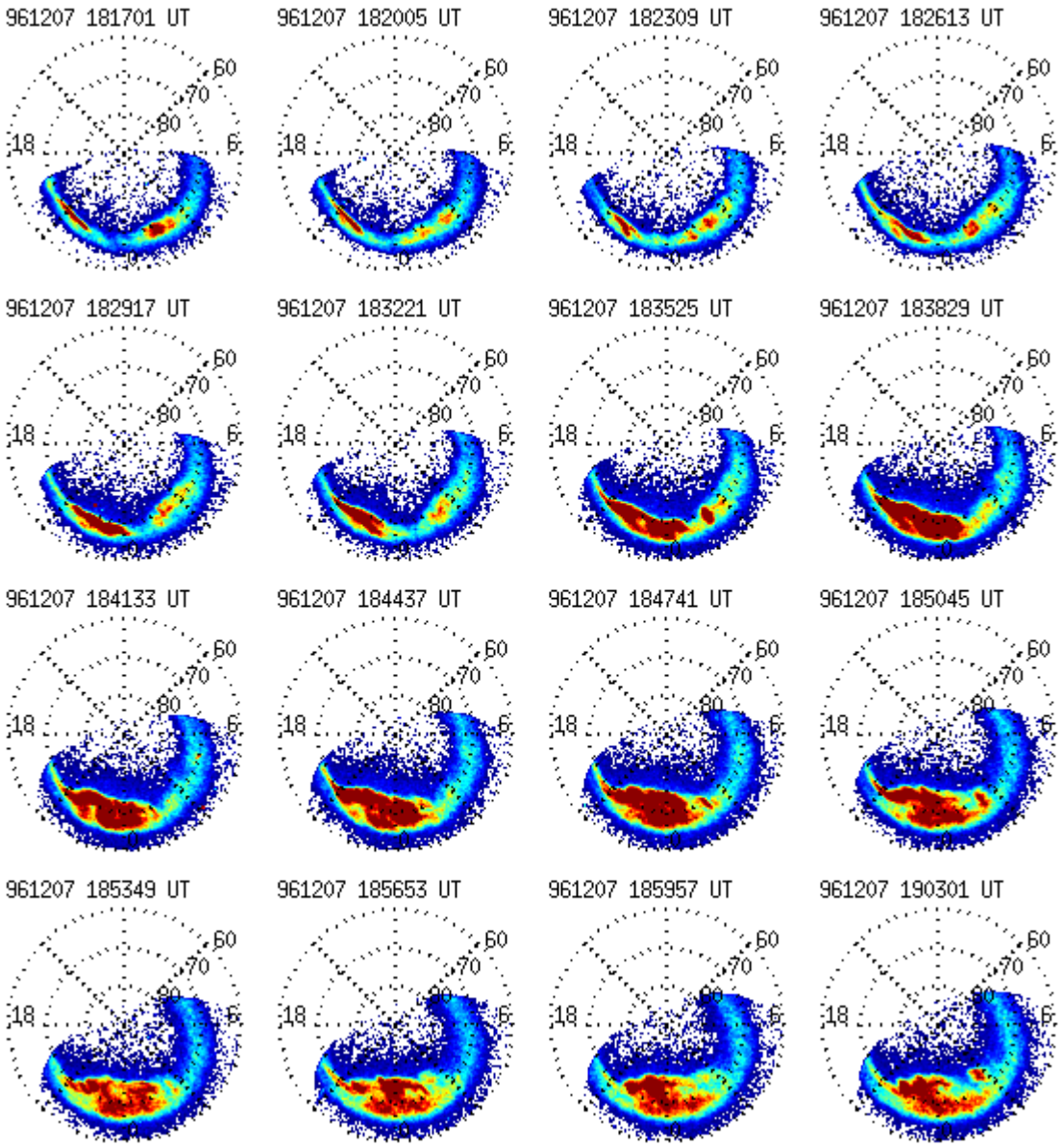

Figure 3. False color images from 18:17 to 19:03 UT on December 7, 1996. Same format as Figure 1 except the scale extends to 30 photons/cm^{2}s.

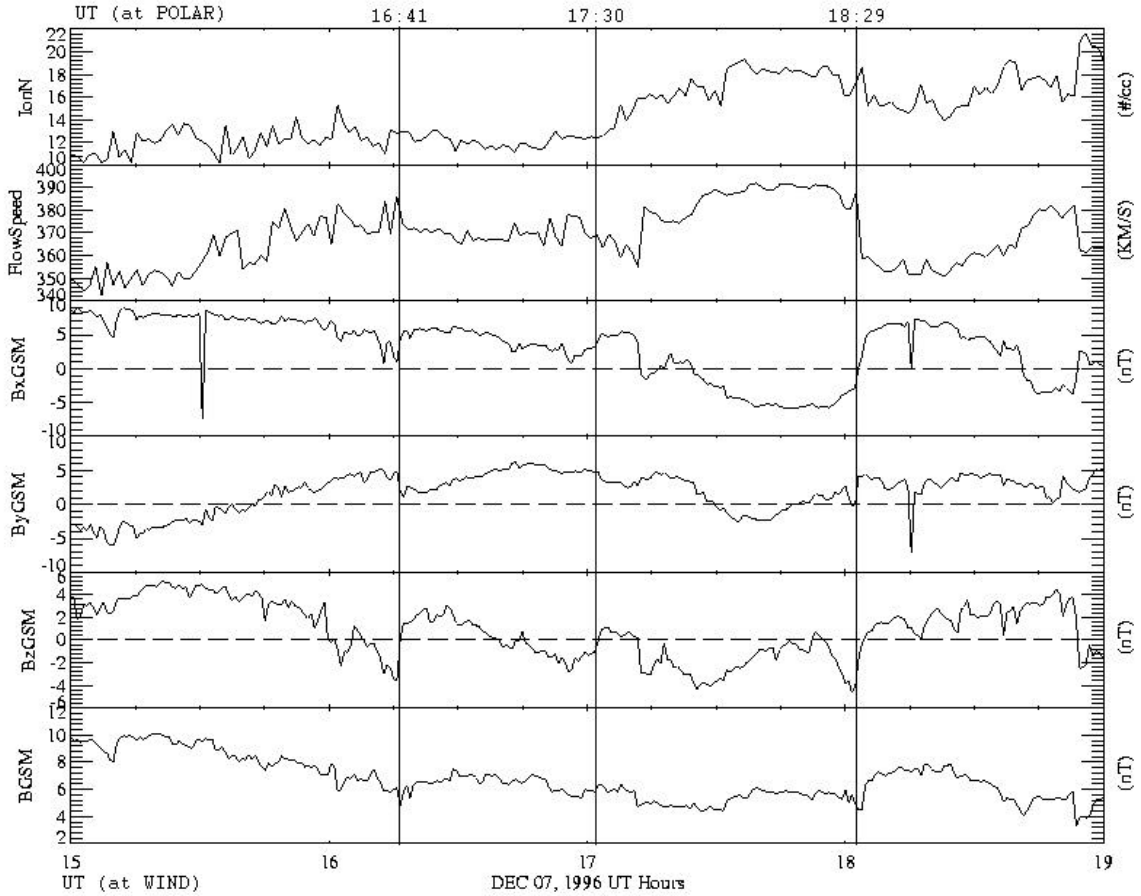

Figure 4 Shows 1-minute averages of solar wind density, velocity and the three components and magnitude of the IMF in the geocentric solar magnetospheric (GSM) coordinate system. Labels at the bottom of the figure are UT, labels at the top are corresponding POLAR UV image time tags which have been time-shifted with respect to UT to account for transit time of the IMF measured at WIND to when the effects are seen in the Earth's ionosphere. For the period under study WIND was located at approximately X=44, Y=-48, Z=5 R_E GSM.

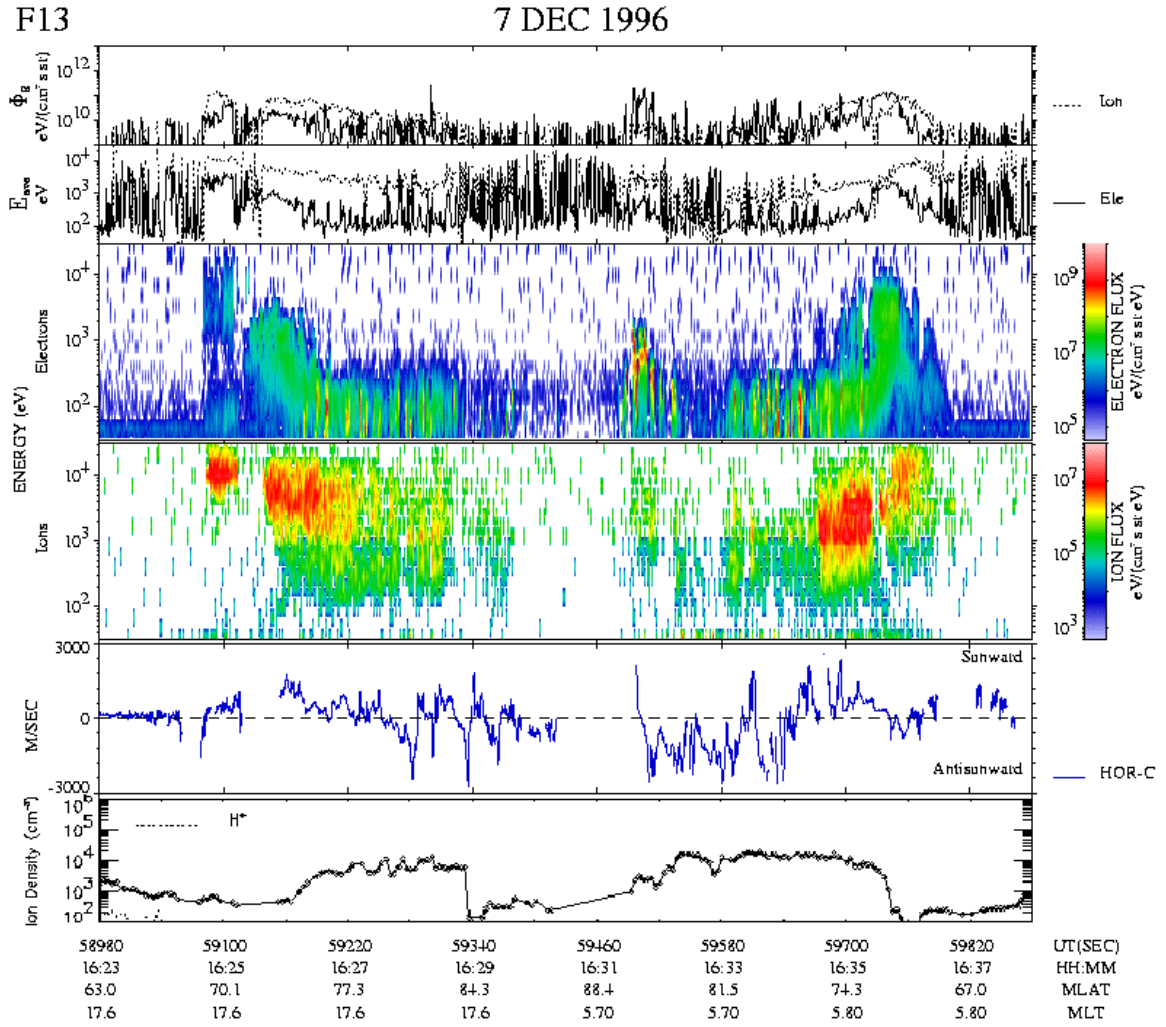

Figure 5 Energetic particle distribution observed by DMSP F13 corresponding to the first image in Figure 1. Shown from top to bottom: (1) electron and ion integral energy flux, (2) electron and ion average energy, (3) precipitating electron spectrogram, (4) precipitating ion spectrogram, (5) cross-track horizontal plasma drift, and (6) ion density. See text for details.

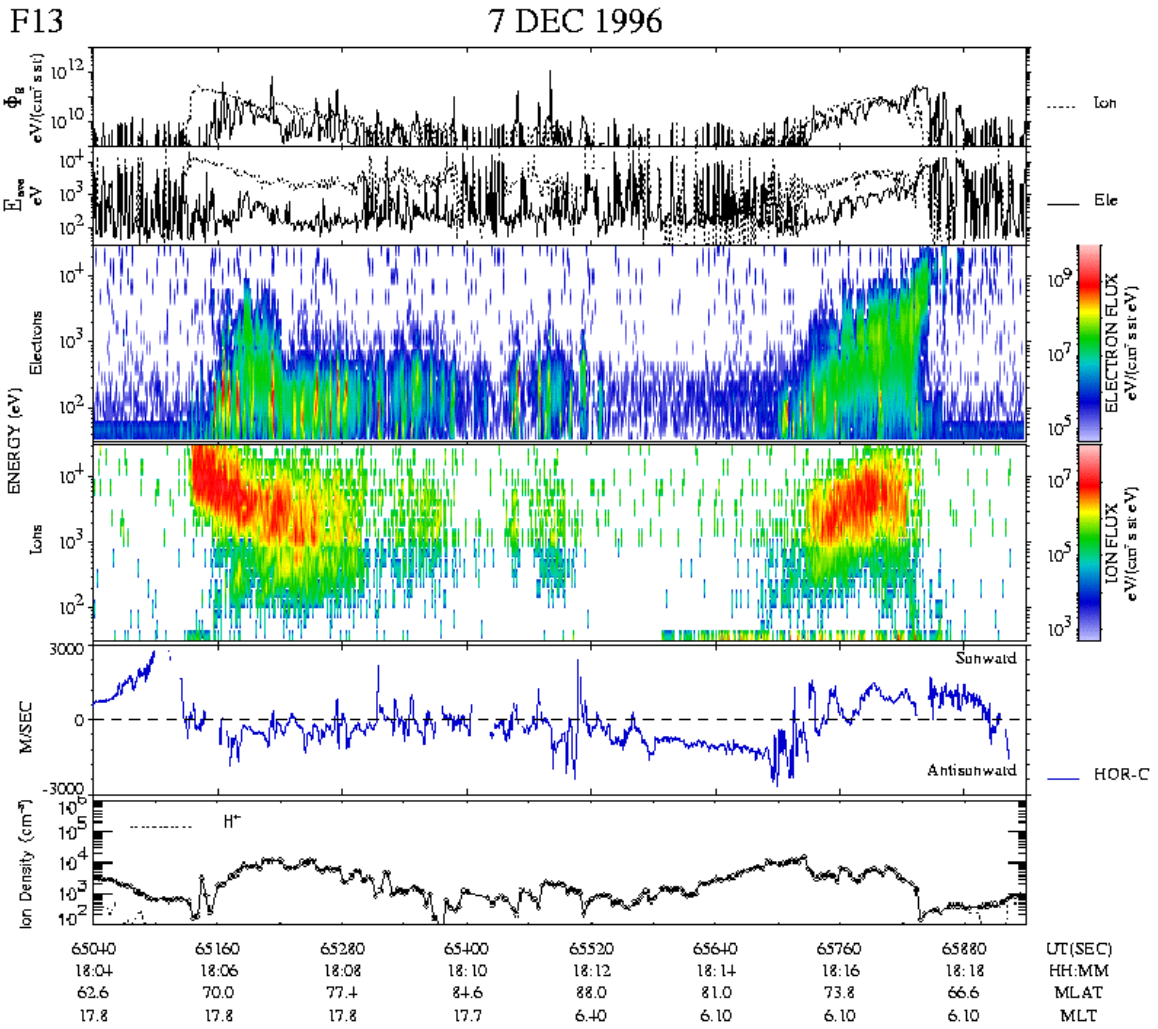

Figure 6. Energetic particle distribution observed by DMSP F13 corresponding to the last image in Figure 2; same format as Figure 5.

TRITA-ALP-2000-01
ISSN 1103-6613

POLAR UVI Observations of Auroral Oval Intensifications During a Transpolar Arc Event on December 7, 1996

J. A. Cumnock, J. F. Spann, G. A. Germany, L. G. Blomberg
W. R. Coley, C. R. Clauer, M. J. Brittnacher

Abstract

The evolution of the northern hemisphere aurora is examined during a time when the IMF makes three brief southward excursions after a change in the sign of B_y during an extended period of northward IMF. POLAR UVI provides images of the aurora while DMSP F13 and F14 provide in situ measurements of precipitating particles, ionospheric plasma flows and ion density.

Three different intensifications located in the nightside auroral oval occur during northward turnings of the IMF after brief periods of southward IMF. Spatial expansion, intensity of emissions and their duration are related to the length of time the IMF is southward prior to the northward turning. Thus the longer the period of enhanced magnetospheric convection the more intense the ionospheric response. Observations of a transpolar arc indicate that when the transpolar arc reaches highest latitudes it is located on a spatially narrow region of closed field lines which extends along the noon-midnight meridian.

UV observations indicate a connection between the transpolar arc and the nightside auroral enhancements. Precipitating particles associated with both features are attributed to a plasma sheet boundary layer source in the magnetotail implying a magnetospheric connection between the transpolar arc and the nightside auroral oval intensification.

21 Pages
6 Figures
Keywords: Auroral Physics, Magnetosphere-ionosphere Coupling, Northward IMF, Substorm, Theta Aurora, Transpolar Arc